

**A method for exact compensation of voltage and current phasors computed by orthogonal FIR filters during frequency variations**

Journal:	<i>Electric Power Components and Systems</i>
Manuscript ID:	Draft
Manuscript Type:	Original Article
Date Submitted by the Author:	n/a
Complete List of Authors:	Apostolopoulos, Christos A.; National Technical University of Athens, Electrical and Computer Engineering Korres, George N.; National Technical University of Athens, Greece, Electrical and Computer Engineering
Keywords:	power system measurement, power system frequency estimation, power system protection, digital relaying, digital/numeric protection

SCHOLARONE™  
Manuscripts

1  
2  
3  
4  
5  
6  
7  
8  
9  
10  
11  
12  
13  
14  
15  
16  
17  
18  
19  
20  
21  
22  
23  
24  
25  
26  
27  
28  
29  
30  
31  
32  
33  
34  
35  
36  
37  
38  
39  
40  
41  
42  
43  
44  
45  
46  
47  
48  
49  
50  
51  
52  
53  
54  
55  
56  
57  
58  
59  
60

‘To remain an Accept with Change manuscript’

# A method for exact compensation of voltage and current phasors computed by orthogonal FIR filters during frequency variations

C. A. Apostolopoulos\*, G. N. Korres

National Technical University of Athens, ECE Department

Iroon Polytechniou 9, Zografou 15780, Athens, Greece

\*Tel: +30 210 7723561, Fax: +30 210 7723659, Email: [apostolo@power.ece.ntua.gr](mailto:apostolo@power.ece.ntua.gr)

**Abstract:** This paper presents a generic method that fully compensates for the errors introduced by orthogonal FIR filters (full-cycle DFT, half-cycle DFT, Cosine filter) in phasor computation during frequency variations in power systems. To accomplish this, the proposed method uses an accurate and easily calculated estimate of the local instantaneous frequency. The method is robust and precise and can be extended to deal satisfactorily with the effect of harmonics. Also its implementation simplicity, makes it attractive for real-time applications. Simulation results are provided to demonstrate the effectiveness of the proposed method.

**Keywords:** Phasor computation, discrete Fourier transform (DFT), orthogonal finite impulse response (FIR) filters, frequency variations, instantaneous frequency estimation, protective relaying, power system measurements.

## 1. Introduction

Accurate phasor measurement is a key task for modern power system protection and control. Microprocessor-based relays use numerical algorithms to extract the fundamental component phasors from their voltage and current inputs. The phasors are then used by protective relays to carry out their monitoring and protection functions. In addition, the algorithm for phasor calculation is the kernel of Phasor Measurement Units (PMUs) which are currently becoming widely available, and are starting to be used in power systems.

Typically, some sort of digital filtering is employed for phasor computation [1]. Among the most popular digital filtering systems are the half and full-cycle discrete Fourier transform (DFT) or its offshoot, the full-cycle Cosine filter. These systems comprise a pair of orthogonal finite impulse response (FIR) filters which are designed to have a

1 unity gain at the rated power system frequency and zero gains at dc and harmonic frequencies, and a phase angle  
2  
3 between their outputs equal to  $90^{\circ}$ .  
4

5 The two FIR filters are applied to a data window of consecutive sample points of a discrete input signal, which has  
6 a sampling frequency that is synchronous with the rated power system frequency. However, if the actual frequency is  
7 different than the rated frequency, the phasors produced by the two filters will have errors, both in magnitude and in  
8 phase angle [2]. These errors can result in improper performance of protective relays [3] and in poor quality of  
9 synchrophasors in PMUs [4].  
10  
11

12 In practice, it is not necessary or likely for the power system to be operating exactly at its rated frequency. Under  
13 normal conditions, the frequency of the power system is constantly varying to a small degree around its rated  
14 frequency. In this case, the phasor measurement errors are typically small. However, under dynamic conditions, the  
15 power system can experience large frequency excursions which can adversely affect the accuracy of phasor  
16 computation by orthogonal FIR filters. The presence of harmonics under these conditions would further aggravate the  
17 problem. Typical examples of such power system conditions are generator startups and disconnections, sudden  
18 applications and losses of large blocks of load and power swings.  
19  
20  
21  
22  
23  
24  
25  
26  
27  
28  
29  
30

31 DFT is the most commonly applied method for fundamental phasor calculation. Thus, most of the developed  
32 compensation techniques aim at cancelling out the errors introduced by DFT during off-nominal frequency operation.  
33 The most popular among them is known as frequency tracking [5]. The frequency tracking mechanism estimates the  
34 local instantaneous frequency [6]-[8], and thereafter modifies the phasor computation process by adjusting one out of  
35 three: 1) the sampling frequency so as to be synchronous with the actual frequency [9], 2) the data window length so  
36 as to correspond to a whole cycle of the actual frequency [10], 3) the FIR filters so as to be tuned to the actual  
37 frequency [11].  
38  
39  
40  
41  
42  
43  
44  
45  
46

47 The above mentioned techniques use the phase angle error created by DFT due to asynchronous sampling for  
48 instantaneous frequency estimation. However, they do not take into account the complete phase angle error. This  
49 results in additional smoothing needed (polynomial fitting [7]-[8], moving average filter [10]) to obtain a correct  
50 frequency estimate, which further delays the frequency tracking process and thus the phasor computation. Only the  
51 smart discrete Fourier transform (SDFT) method [12] takes into account the DFT errors completely. The results  
52 obtained by SDFT for both frequency and phasor estimation are very good, but the method is rather complicated to  
53  
54  
55  
56  
57  
58  
59  
60

calculate especially in the presence of harmonics. Moreover, SDFT is applicable only to full-cycle Fourier-type FIR filters.

There are also several other non-DFT based methods for phasor computation (such as Kalman filter [13], recursive least squares [14], Newton method [15], complex Taylor's series expansion [16]-[17] etc.), which are reported in the literature and can provide satisfactory phasor estimates under dynamic conditions. However, techniques such as DFT, which utilize a pair of orthogonal FIR filters for determining the measured phasor, are the predominant ones in currently available protective relays and PMUs due to their low computational cost and simplicity, and this is a motivation for further research to enhance their performance under frequency variations.

This paper contributes to this direction. It uses a precise and easily calculated estimate of the local instantaneous frequency to fully compensate for the errors introduced in phasor computation during frequency variations. The method is applicable to any filtering system which comprises two orthogonal FIR filters, including particularly Fourier and Cosine filter, but other FIR filters or combination thereof as well. It thus has the advantage of wide applicability. The theoretical basis of the proposed phasor compensation method are presented in Section 2. The method is validated by three examples in Section 3. In Section 4, the method is extended to deal with the problem of harmonics.

## 2. Theoretical analysis

### 2.1. The phasor compensation method

Consider a sinusoidal input signal  $x(t)$  of the form:

$$x(t) = A \cos(\delta(t)) \quad (1)$$

where  $A$  is the amplitude and  $\delta(t)$  is the time-varying phase angle of the input signal.

The instantaneous frequency of the input signal, according to the definition given in [6]-[8], is:

$$f(t) = \frac{1}{2\pi} \frac{d\delta(t)}{dt}. \quad (2)$$

Using (2) in (1),  $x(t)$  can be expressed as:

$$x(t) = A \cos(2\pi \int_0^t f(\tau) d\tau + \phi). \quad (3)$$

where  $\phi$  is the initial phase angle of the input signal with respect to an arbitrary reference.

Let us assume that  $x(t)$  is sampled  $N$  times the rated power system frequency  $f_N$ . Then, a sample  $x[k]$  is defined as follows:

$$x[k] = x(k\Delta T) = A\cos(\delta(k\Delta T)) = A\cos(\delta[k]) \quad (4)$$

where  $\Delta T = 1/(Nf_N)$  is the sampling period and  $k = 0, 1, 2, \dots$  is the sample number. Moreover,  $x[k]$  can be written as:

$$x[k] = \left( Ae^{j\delta[k]} + Ae^{-j\delta[k]} \right) / 2. \quad (5)$$

Generally, the fundamental component phasor,  $\overline{X}_m$ , of  $\{x[k]\}$  at time sample  $r$  is computed using the following formula:

$$\overline{X}_m[r] = \sum_{n=0}^{N-1} x[r+n](a_n + jb_n) \quad (6)$$

where  $a_n$  and  $b_n$  are the coefficients of the two FIR filters, which are constant real numbers and are associated with the type of filter used.

For example, for a full cycle DFT filter pair, the coefficients of the FIR filters are:

$$a_n + jb_n = \frac{2}{N} e^{-j\frac{2\pi n}{N}} = \frac{2}{N} \left( \cos\left(\frac{2\pi n}{N}\right) - j \sin\left(\frac{2\pi n}{N}\right) \right) = \frac{2}{N} e^{-j2\pi n f_N \Delta T} \quad (7)$$

$$n = 0, 1, \dots, N-1$$

For a half-cycle DFT filter, that has data windows which are one-half of the full cycle DFT, the coefficients of the corresponding FIR filters are provided by the following formula:

$$a_n + jb_n = \frac{4}{N} e^{-j\frac{2\pi n}{N}} = \frac{4}{N} \left( \cos\left(\frac{2\pi n}{N}\right) - j \sin\left(\frac{2\pi n}{N}\right) \right) = \frac{4}{N} e^{-j2\pi n f_N \Delta T} \quad (8)$$

$$n = 0, 1, \dots, N/2 - 1$$

For a full cycle Cosine filter, which exhibits a better rejection than the Fourier filter for any exponentially decaying component present in current signals during a fault, the measured phasor is given by the following equation:

$$\overline{X}_m[r] = \frac{2}{N} \sum_{n=0}^{N-1} (x[r+n] + jx[r+n-N/4]) \cos\left(\frac{2\pi n}{N}\right) = \frac{1}{N} \sum_{n=0}^{N-1} (x[r+n] + jx[r+n-N/4]) \left( e^{-j2\pi n f_N \Delta T} + e^{j2\pi n f_N \Delta T} \right) \quad (9)$$

$$n = 0, 1, \dots, N-1$$

Combining (5) and (6), we have:

$$\overline{X}_m[r] = \frac{A}{2} \sum_{n=0}^{N-1} e^{j\delta[r+n]} (a_n + jb_n) + \frac{A}{2} \sum_{n=0}^{N-1} e^{-j\delta[r+n]} (a_n + jb_n). \quad (10)$$

In practice, is not feasible to calculate the summations in (10) due to the term  $\delta[r+n]$ . It is obvious that some sort of approximation must be used in forming this term. The linear interpolation scheme can be applied, assuming that the phase angle is varying linearly between two consecutive sampling time instants,  $r\Delta T$  and  $(r+1)\Delta T$ . On this basis, the term  $\delta[r+n]$  is given by:

$$\delta[r+n] = \delta[r] + \frac{\delta[r+1] - \delta[r]}{(r+1)\Delta T - r\Delta T} ((r+n)\Delta T - r\Delta T) = \delta[r] + \frac{\delta[r+1] - \delta[r]}{\Delta T} n\Delta T. \quad (11)$$

Substituting (11) in (10), we obtain:

$$\overline{X}_m[r] = \frac{A}{2} e^{j\delta[r]} \sum_{n=0}^{N-1} e^{j2\pi \left( \frac{1}{2\pi} \frac{\delta[r+1] - \delta[r]}{\Delta T} \right) n\Delta T} (a_n + jb_n) + \frac{A}{2} e^{-j\delta[r]} \sum_{n=0}^{N-1} e^{-j2\pi \left( \frac{1}{2\pi} \frac{\delta[r+1] - \delta[r]}{\Delta T} \right) n\Delta T} (a_n + jb_n). \quad (12)$$

Equation (12) can be rewritten as:

$$\overline{X}_m[r] = \frac{A}{2} e^{j\delta[r]} \sum_{n=0}^{N-1} e^{j2\pi \hat{f}[r] n\Delta T} (a_n + jb_n) + \frac{A}{2} e^{-j\delta[r]} \sum_{n=0}^{N-1} e^{-j2\pi \hat{f}[r] n\Delta T} (a_n + jb_n) \quad (13)$$

where  $\hat{f}[r]$  is an estimate of the instantaneous frequency according to (2):

$$\hat{f}[r] = \frac{1}{2\pi} \frac{\delta[r+1] - \delta[r]}{\Delta T}. \quad (14)$$

Let the exact phasor  $\overline{X}$  of the sinusoidal input signal at time sample  $r$  be denoted:

$$\overline{X}[r] = Ae^{j\delta[r]}. \quad (15)$$

Using (15) and the following identity:

$$\sum_{n=0}^{N-1} \left( e^{j\theta} \right)^n = \frac{\sin \frac{N\theta}{2}}{\sin \frac{\theta}{2}} e^{j(N-1)\frac{\theta}{2}} \quad (16)$$

equation (13) can be expressed as:

$$\overline{X}_m[r] = \overline{P}(\hat{f}[r]) \overline{X}[r] + \overline{Q}(\hat{f}[r]) \overline{X}^*[r] \quad (17)$$

where  $*$  denotes complex conjugate and  $\overline{P}$ ,  $\overline{Q}$  are two correction factors, which are functions of the instantaneous frequency  $\hat{f}$  and are defined for each particular filter arrangement as follows:

$$\text{full-cycle DFT: } \begin{cases} \bar{P}_{DFT}(\hat{f}[r]) = \frac{\sin(\pi N(\hat{f}[r] - f_N)\Delta T)}{N \sin(\pi(\hat{f}[r] - f_N)\Delta T)} e^{j(N-1)(\pi(\hat{f}[r] - f_N)\Delta T)} \\ \bar{Q}_{DFT}(\hat{f}[r]) = \frac{\sin(\pi N(\hat{f}[r] + f_N)\Delta T)}{N \sin(\pi(\hat{f}[r] + f_N)\Delta T)} e^{-j(N-1)(\pi(\hat{f}[r] + f_N)\Delta T)} \end{cases} \quad (18)$$

$$\text{half-cycle DFT: } \begin{cases} \bar{P}_{HCFT}(\hat{f}[r]) = \frac{2 \sin(\pi N(\hat{f}[r] - f_N)\Delta T)}{N \sin(\pi(\hat{f}[r] - f_N)\Delta T)} e^{j(\frac{N}{2}-1)(\pi(\hat{f}[r] - f_N)\Delta T)} \\ \bar{Q}_{HCFT}(\hat{f}[r]) = \frac{2 \sin(\pi N(\hat{f}[r] + f_N)\Delta T)}{N \sin(\pi(\hat{f}[r] + f_N)\Delta T)} e^{-j(\frac{N}{2}-1)(\pi(\hat{f}[r] + f_N)\Delta T)} \end{cases} \quad (19)$$

Cosine filter:

$$\begin{cases} \bar{P}_{Cos}(\hat{f}[r]) = \frac{1}{2N} \left( 1 + je^{-j\frac{N\pi\hat{f}[r]\Delta T}{2}} \left( \frac{\sin(\pi N(\hat{f}[r] - f_N)\Delta T)}{\sin(\pi(\hat{f}[r] - f_N)\Delta T)} e^{j(N-1)(\pi(\hat{f}[r] - f_N)\Delta T)} + \frac{\sin(\pi N(\hat{f}[r] + f_N)\Delta T)}{\sin(\pi(\hat{f}[r] + f_N)\Delta T)} e^{j(N-1)(\pi(\hat{f}[r] + f_N)\Delta T)} \right) \right) \\ \bar{Q}_{Cos}(\hat{f}[r]) = \frac{1}{2N} \left( 1 + je^{j\frac{N\pi\hat{f}[r]\Delta T}{2}} \left( \frac{\sin(\pi N(\hat{f}[r] - f_N)\Delta T)}{\sin(\pi(\hat{f}[r] - f_N)\Delta T)} e^{-j(N-1)(\pi(\hat{f}[r] - f_N)\Delta T)} + \frac{\sin(\pi N(\hat{f}[r] + f_N)\Delta T)}{\sin(\pi(\hat{f}[r] + f_N)\Delta T)} e^{-j(N-1)(\pi(\hat{f}[r] + f_N)\Delta T)} \right) \right) \end{cases} \quad (20)$$

If we write  $\bar{P}$ ,  $\bar{Q}$ ,  $\bar{X}_m$  and  $\bar{X}$  in (17) in terms of their real and imaginary parts:  $\bar{P} = P_R + jP_I$ ,  $\bar{Q} = Q_R + jQ_I$ ,

$\bar{X}_m = X_{mR} + jX_{mI}$  and  $\bar{X} = X_R + jX_I$ , we obtain:

$$\begin{pmatrix} X_{mR}[r] \\ X_{mI}[r] \end{pmatrix} = \begin{pmatrix} P_R(\hat{f}[r]) + Q_R(\hat{f}[r]) & Q_I(\hat{f}[r]) - P_I(\hat{f}[r]) \\ P_I(\hat{f}[r]) + Q_I(\hat{f}[r]) & P_R(\hat{f}[r]) - Q_R(\hat{f}[r]) \end{pmatrix} \begin{pmatrix} X_R[r] \\ X_I[r] \end{pmatrix}. \quad (21)$$

The exact phasor can be calculated as:

$$\begin{pmatrix} X_R[r] \\ X_I[r] \end{pmatrix} = \begin{pmatrix} P_R(\hat{f}[r]) + Q_R(\hat{f}[r]) & Q_I(\hat{f}[r]) - P_I(\hat{f}[r]) \\ P_I(\hat{f}[r]) + Q_I(\hat{f}[r]) & P_R(\hat{f}[r]) - Q_R(\hat{f}[r]) \end{pmatrix}^{-1} \begin{pmatrix} X_{mR}[r] \\ X_{mI}[r] \end{pmatrix}. \quad (22)$$

Since the instantaneous frequency  $\hat{f}$  is required at each sample time  $r$  for computing the exact phasor in (22), it must be calculated first. This can be done using the procedure described in the next paragraph.

## 2.2. Calculation of the instantaneous frequency $\hat{f}$

According to (10), the fundamental component phasor at time sample  $r-1$  is given by:

$$\bar{X}_m[r-1] = \frac{A}{2} \sum_{n=0}^{N-1} e^{j\delta[r-1+n]} (a_n + jb_n) + \frac{A}{2} \sum_{n=0}^{N-1} e^{-j\delta[r-1+n]} (a_n + jb_n). \quad (23)$$

Applying the linear interpolation scheme performed in (11) for the term  $\delta[r-1+n]$  and substituting in (23), we

obtain:

$$\overline{X}_m[r-1] = \frac{A}{2} e^{j\delta(r)} e^{-j2\pi\left(\frac{1}{2\pi}\frac{\delta[r+1]-\delta[r]}{\Delta T}\right)\Delta T} \cdot \sum_{n=0}^{N-1} e^{j2\pi\left(\frac{1}{2\pi}\frac{\delta[r+1]-\delta[r]}{\Delta T}\right)n\Delta T} (a_n + jb_n) + \frac{A}{2} e^{-j\delta(r)} e^{j2\pi\left(\frac{1}{2\pi}\frac{\delta[r+1]-\delta[r]}{\Delta T}\right)\Delta T} \cdot \sum_{n=0}^{N-1} e^{-j2\pi\left(\frac{1}{2\pi}\frac{\delta[r+1]-\delta[r]}{\Delta T}\right)n\Delta T} (a_n + jb_n). \quad (24)$$

Combining (14), (15), (16), (17) and (24), we have:

$$\overline{X}_m[r-1] = e^{-j2\pi\hat{f}[r]\Delta T} \overline{P}(\hat{f}[r])\overline{X}[r] + e^{j2\pi\hat{f}[r]\Delta T} \overline{Q}(\hat{f}[r])\overline{X}^*[r]. \quad (25)$$

Following a similar procedure as above, the fundamental component phasor at time sample  $r-2$  can be expressed as:

$$\overline{X}_m[r-2] = e^{-j2(2\pi\hat{f}[r]\Delta T)} \overline{P}(\hat{f}[r])\overline{X}[r] + e^{j2(2\pi\hat{f}[r]\Delta T)} \overline{Q}(\hat{f}[r])\overline{X}^*[r]. \quad (26)$$

Let  $\overline{z}$  be defined as:

$$\overline{z} = e^{j2\pi\hat{f}[r]\Delta T}. \quad (27)$$

Using (27) in (25) and (26) and multiplying  $\overline{X}_m[r]$  with  $\overline{X}_m^*[r-1]$  and  $\overline{X}_m^*[r-2]$  respectively, we get:

$$\begin{aligned} \overline{X}_m[r] \cdot \overline{X}_m^*[r-1] &= \left( \overline{P}(\hat{f}[r])\overline{X}[r] + \overline{Q}(\hat{f}[r])\overline{X}^*[r] \right) \cdot \left( \overline{z} \overline{P}(\hat{f}[r])\overline{X}^*[r] + \overline{z}^{-1} \overline{Q}(\hat{f}[r])\overline{X}[r] \right) \\ &= \overline{z} \left| \overline{P}(\hat{f}[r]) \right|^2 \left| \overline{X}[r] \right|^2 + \overline{z}^{-1} \overline{P}(\hat{f}[r])\overline{Q}(\hat{f}[r]) \left( \overline{X}[r] \right)^2 + \overline{z} \overline{P}(\hat{f}[r])\overline{Q}(\hat{f}[r]) \left( \overline{X}^*[r] \right)^2 + \overline{z}^{-1} \left| \overline{Q}(\hat{f}[r]) \right|^2 \left| \overline{X}[r] \right|^2 \end{aligned} \quad (28)$$

$$\begin{aligned} \overline{X}_m[r] \cdot \overline{X}_m^*[r-2] &= \left( \overline{P}(\hat{f}[r])\overline{X}[r] + \overline{Q}(\hat{f}[r])\overline{X}^*[r] \right) \cdot \left( \overline{z}^2 \overline{P}(\hat{f}[r])\overline{X}^*[r] + \overline{z}^{-2} \overline{Q}(\hat{f}[r])\overline{X}[r] \right) \\ &= \overline{z}^2 \left| \overline{P}(\hat{f}[r]) \right|^2 \left| \overline{X}[r] \right|^2 + \overline{z}^{-2} \overline{P}(\hat{f}[r])\overline{Q}(\hat{f}[r]) \left( \overline{X}[r] \right)^2 + \overline{z}^2 \overline{P}(\hat{f}[r])\overline{Q}(\hat{f}[r]) \left( \overline{X}^*[r] \right)^2 + \overline{z}^{-2} \left| \overline{Q}(\hat{f}[r]) \right|^2 \left| \overline{X}[r] \right|^2. \end{aligned} \quad (29)$$

Taking the complex conjugate on the left hand side of (28) and (29), we have:

$$\overline{X}_m^*[r] \cdot \overline{X}_m[r-1] = \overline{z}^{-1} \left| \overline{P}(\hat{f}[r]) \right|^2 \left| \overline{X}[r] \right|^2 + \overline{z}^{-1} \overline{P}(\hat{f}[r])\overline{Q}(\hat{f}[r]) \left( \overline{X}[r] \right)^2 + \overline{z} \overline{P}(\hat{f}[r])\overline{Q}(\hat{f}[r]) \left( \overline{X}^*[r] \right)^2 + \overline{z} \left| \overline{Q}(\hat{f}[r]) \right|^2 \left| \overline{X}[r] \right|^2 \quad (30)$$

$$\overline{X}_m^*[r] \cdot \overline{X}_m[r-2] = \overline{z}^{-2} \left| \overline{P}(\hat{f}[r]) \right|^2 \left| \overline{X}[r] \right|^2 + \overline{z}^{-2} \overline{P}(\hat{f}[r])\overline{Q}(\hat{f}[r]) \left( \overline{X}[r] \right)^2 + \overline{z}^2 \overline{P}(\hat{f}[r])\overline{Q}(\hat{f}[r]) \left( \overline{X}^*[r] \right)^2 + \overline{z}^2 \left| \overline{Q}(\hat{f}[r]) \right|^2 \left| \overline{X}[r] \right|^2. \quad (31)$$

Subtracting (30) from (28) and (31) from (29) respectively, we obtain:

$$\overline{X}_m[r] \cdot \overline{X}_m^*[r-1] - \overline{X}_m^*[r] \cdot \overline{X}_m[r-1] = \left( \overline{z} - \overline{z}^{-1} \right) \left( \left| \overline{P}(\hat{f}[r]) \right|^2 - \left| \overline{Q}(\hat{f}[r]) \right|^2 \right) \left| \overline{X}[r] \right|^2 \quad (32)$$

$$\overline{X}_m[r] \cdot \overline{X}_m^*[r-2] - \overline{X}_m^*[r] \cdot \overline{X}_m[r-2] = \left( \overline{z}^2 - \overline{z}^{-2} \right) \left( \left| \overline{P}(\hat{f}[r]) \right|^2 - \left| \overline{Q}(\hat{f}[r]) \right|^2 \right) \left| \overline{X}[r] \right|^2. \quad (33)$$

Dividing (33) by (32) and using (27), we get:

$$\frac{\overline{X_m[r]} \cdot \overline{X_m^*[r-2]} - \overline{X_m^*[r]} \cdot \overline{X_m[r-2]}}{\overline{X_m[r]} \cdot \overline{X_m^*[r-1]} - \overline{X_m^*[r]} \cdot \overline{X_m[r-1]}} = \frac{\overline{z}^{-2} - \overline{z}^{-2}}{\overline{z} - \overline{z}^{-1}} = \frac{\overline{z}^{-2}}{\overline{z} + \overline{z}^{-1}}. \quad (34)$$

Equation (34) can be expressed in Cartesian components, using the definition of  $\overline{z}$  in (27), as:

$$\frac{X_{ml}[r]X_{mR}[r-2] - X_{mR}[r]X_{ml}[r-2]}{X_{ml}[r]X_{mR}[r-1] - X_{mR}[r]X_{ml}[r-1]} = 2\text{Re}\left(\frac{\overline{z}}{\overline{z} + \overline{z}^{-1}}\right). \quad (35)$$

From (27) and (35), we can obtain the solution of the instantaneous frequency  $\hat{f}$  at each time sample  $r$ . It is:

$$\hat{f}[r] = \frac{1}{2\pi\Delta T} \cos^{-1}\left(\frac{X_{ml}[r]X_{mR}[r-2] - X_{mR}[r]X_{ml}[r-2]}{2(X_{ml}[r]X_{mR}[r-1] - X_{mR}[r]X_{ml}[r-1])}\right). \quad (36)$$

After computing  $\hat{f}[r]$ , we can compute the exact fundamental component phasor by (22).

### 3. Method validation

#### 3.1. Computational issues

Several simulation studies have been conducted in Matlab to validate the proposed method. In all test cases the sampling frequency is 800 Hz, the data window length is  $N=16$  and the rated frequency  $f_N$  is assumed to be 50 Hz. Moreover, the unavoidable quantization error of the input signal due to the analog-digital conversion (ADC) has been simulated as:

$$y[k] = 2^{-M} \cdot \text{round}\left(x[k]/2^{-M}\right), \quad k = 0, 1, 2, \dots, \quad (37)$$

where  $M = 16$  bits is the word length of the ADC assumed.

The elements of the inverse 2x2 matrix in (22) can be precalculated for several frequency differences  $\Delta\hat{f} = \hat{f} - f_N$ , in order to speed up the computation of the exact phasor. This can be done by rewriting (22) in the following form:

$$\begin{pmatrix} X_R(r) \\ X_I(r) \end{pmatrix} = \begin{pmatrix} A(\Delta\hat{f}[r]) & B(\Delta\hat{f}[r]) \\ C(\Delta\hat{f}[r]) & D(\Delta\hat{f}[r]) \end{pmatrix} \begin{pmatrix} X_{mR}[r] \\ X_{ml}[r] \end{pmatrix} \quad (38)$$

where the elements  $A$ ,  $B$ ,  $C$  and  $D$  can be represented by a polynomial of order  $m$ , whose coefficients are obtained by applying the regression analysis of [18] over a preselected range of frequency differences  $\Delta\hat{f}$ . In a real-time implementation scheme, the four elements values can be stored in a look-up table and can be directly provided once a  $\Delta\hat{f}$  is determined through (36). Fig. 1 shows the plots of the elements  $A$ ,  $B$ ,  $C$  and  $D$ , with respect to a fifth-

order polynomial regression, for each FIR filter pair (half- and full-DFT, Cosine filter) over a frequency deviation range of  $(-20$  to  $+20)$  Hz, as used in all test cases.

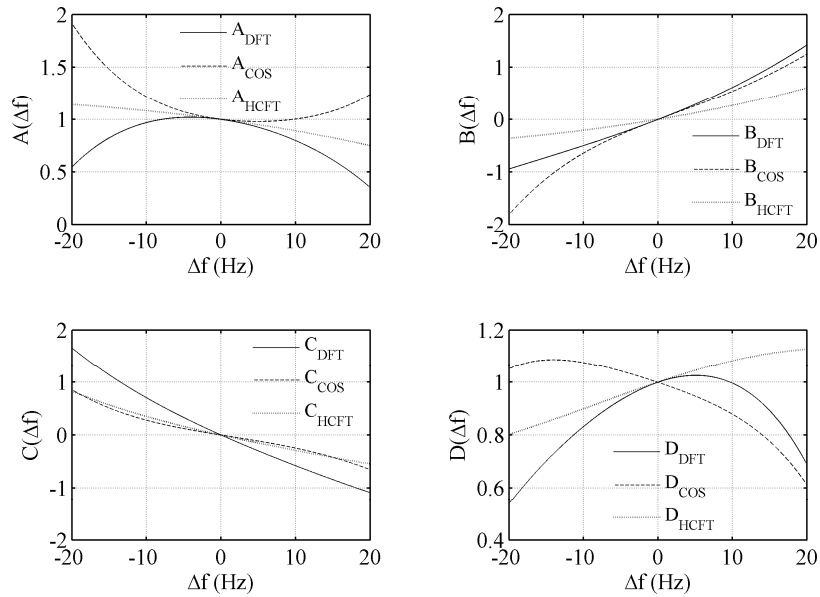


**Fig. 1.** Elements  $A, B, C$ , and  $D$  as a function of frequency deviation  $\Delta \hat{f}$ .

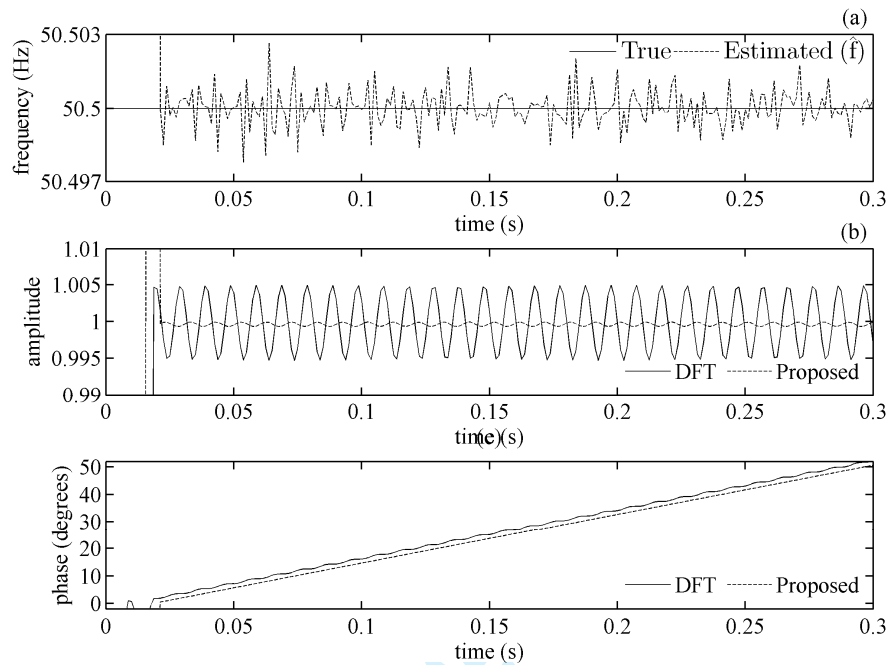
Furthermore, since the fundamental component phasors computed by orthogonal FIR filters and the proposed compensation method are rotating in their nature, they can be made stationary by multiplying the phasors computed in (6) and (22) by  $e^{-j2\pi f_n r \Delta T}$  for each sampling interval  $r$ . Then, the phase angles of the stationary phasors will have only a term relating both to initial phase angle and off-nominal frequency operation:  $2\pi \Delta f t + \phi$ . This will help to observe the changes that the stationary phasors undergo due to off-nominal frequencies in terms of their phase angles.

### 3.2. Simulation results

Three cases are simulated to verify the effectiveness of the proposed method: a constant frequency deviation from the rated frequency, a frequency variation like a ramp and a frequency variation like a sinusoidal.

Fig. 2 corresponds to a typical frequency deviation of  $+0.5$  Hz. The full-cycle DFT filter pair is utilized for fundamental phasor computation. Fig. 3 corresponds to a frequency variation like a ramp from 50 Hz to 51 Hz in a period of 0.5 s; this 2 Hz/s ramp frequency change is a typical value arising in a power system during a sudden loss of load. This second case is for a full-cycle Cosine filter pair. Fig. 4 corresponds to a frequency variation like a sine

1 wave in a period of 0.5 s, and is a good representation of the frequency modulation encountered in power systems  
 2 during low-frequency oscillations. In this case, a half-cycle DFT filter is adopted for phasor calculation. The test  
 3 signal is a pure sinusoid of the form:  $x(t) = \cos(\delta(t))$ . The existence of higher order harmonics will be examined in  
 4 the following section.  
 5  
 6  
 7  
 8  
 9



33 **Fig. 2.** (a) True and estimated frequency  $\hat{f}$ . (b) Comparison of amplitude computation performances of the full-  
 34 cycle DFT and the proposed method. (c) Comparison of phase angle computation performances of the full-cycle DFT  
 35 and the proposed method (test signal:  $x(t)=\cos(2\pi 50.5t)$ ,  $f(t)=50.5$  Hz).  
 36  
 37  
 38  
 39

40 Fig. 2(a), shows the comparison between the true and the estimated frequency  $\hat{f}$  for the case of a constant  
 41 frequency deviation. It is to be noted that  $\hat{f}$  provides a precise measurement of the actual signal frequency with a  
 42 maximum error less than 0.003 Hz. Fig. 2(b) shows the comparison of amplitude computation performance between  
 43 the full-cycle DFT and the proposed compensation method. We can see that the proposed method can effectively  
 44 eliminate the error produced by the full-cycle DFT, which has the form of a ripple around the actual signal amplitude.  
 45 Moreover, the proposed method can cancel out the error introduced by the full-cycle DFT in phase angle calculation.  
 46 This error has the form of a small variation superimposed on an average slope corresponding to  $2\pi\Delta f t$ , as illustrated  
 47 in Fig. 2(c).  
 48  
 49  
 50  
 51  
 52  
 53  
 54  
 55  
 56  
 57  
 58  
 59  
 60

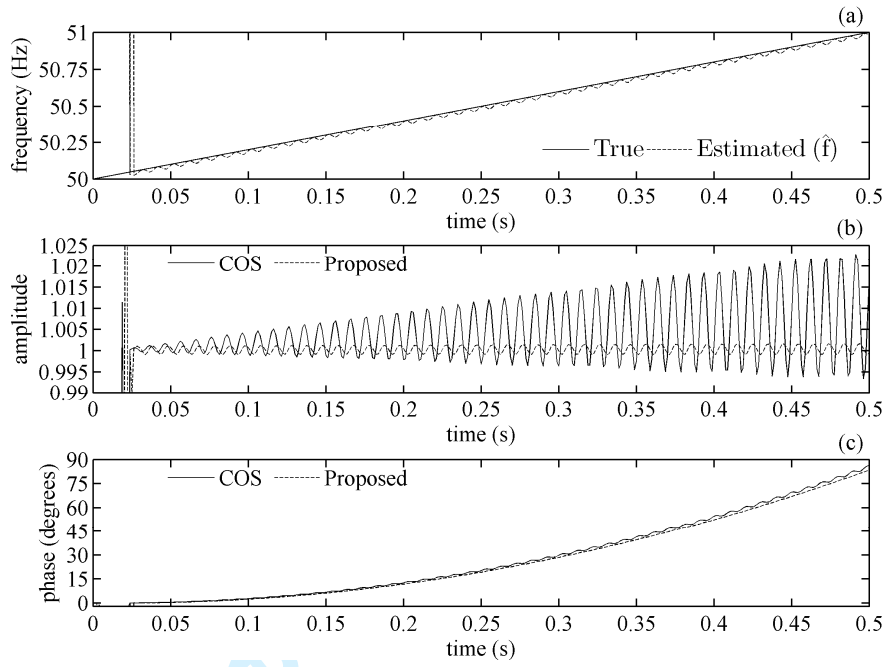


**Fig. 3.** (a) True and estimated frequency  $\hat{f}$  (b) Comparison of amplitude computation performances of the Cosine filter and the proposed method. (c) Comparison of phase angle computation performances of the Cosine filter and the proposed method (test signal:  $x(t)=\cos(2\pi 50t+2\pi t^2)$ ,  $f(t)=50+2t$  Hz).

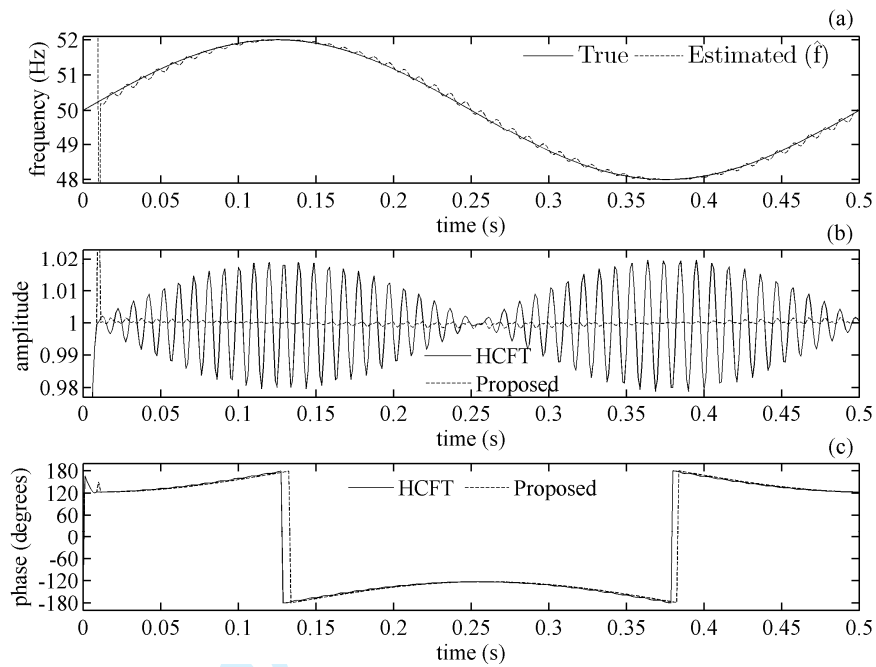


**Fig. 4.** (a) True and estimated frequency  $\hat{f}$ . (b) Comparison of amplitude computation performances of the half-cycle DFT and the proposed method. (c) Comparison of phase angle computation performances of the half-cycle DFT and the proposed method (test signal:  $x(t) = \cos(2\pi 50t - \cos(4\pi t))$ ,  $f(t) = 50 + 2\sin(4\pi t)$  Hz).

Similar observations can be carried out by examining the simulation results depicted in Fig. 3 and 4. Fig. 3(a) and 4(a) show that the tracking performance of  $\hat{f}$  is very satisfactory under dynamic conditions. Fig. 3(b) and 4(b) show that the proposed compensation method gives correct amplitude estimates during dynamic frequency variations, while the Cosine and half-cycle DFT filter pairs give erroneous estimates which are getting worse as the signal frequency deviates further from its rated value. The same holds for the phase angle estimates as can be seen in Fig. 3(c) and 4(c).

In all simulation examples, the proposed method has an additional time lag of one-eighth of the time required by each FIR filter pair to provide a phasor estimate. This time lag is equal to the time needed for obtaining a solution for  $\hat{f}$  by (36) and it is superseded by the accuracy of the phasor estimates obtained.

#### 4. Treatment of harmonics

The hypothesis of a pure sinusoidal input signal is an ideal situation which rarely occurs in practice, especially in modern distribution power systems where power electronic devices have notably increase the level of harmonics. The proposed compensation method can be extended to deal also with the problem of harmonics using a practical and

concise approach, as the one presented in the following paragraphs. In these paragraphs, we will show the modifications needed to include one or more harmonics in the proposed method. Two test cases will demonstrate the feasibility and precision of the extended method.

#### 4.1. Inclusion of a single harmonic

Let us consider a sinusoidal input signal of time-varying frequency  $f(t)$  with  $k$  th harmonic as follows:

$$x(t) = A_1 \cos(2\pi \int_0^t f(\tau) d\tau + \phi_1) + A_k \cos(2\pi k \int_0^t f(\tau) d\tau + \phi_k) \quad (39)$$

where  $A_1, A_k$  and  $\phi_1, \phi_k$  are the amplitudes and initial phase angles of the fundamental and the  $k$  th harmonic component of the input signal.

Based on the analysis of section 2, the phasor  $\overline{X}_m$  computed by orthogonal FIR filters at each sample time  $r$  is given by an expression similar to (17):

$$\overline{X}_m[r] = \overline{P}_1(\hat{f}[r])\overline{X}_1[r] + \overline{Q}_1(\hat{f}[r])\overline{X}_1^*[r] + \overline{P}_k(\hat{f}[r])\overline{X}_k[r] + \overline{Q}_k(\hat{f}[r])\overline{X}_k^*[r] \quad (40)$$

where

$\overline{X}_1$  and  $\overline{X}_k$  : are the exact phasors corresponding to the fundamental and the  $k$  th harmonic respectively;

$\overline{P}_1$  and  $\overline{Q}_1$  : are the correction factor corresponding to the fundamental component, given by (18)-(20) for each type of filter used;

$\overline{P}_k$  and  $\overline{Q}_k$  : are the correction factors corresponding to the  $k$  th harmonic, which are given for each FIR filter pair as:

$$\text{full-cycle DFT: } \begin{cases} \overline{P}_{k_{DFT}}(\hat{f}[r]) = \frac{\sin(\pi N(k\hat{f}[r] - f_N)\Delta T)}{N \sin(\pi(k\hat{f}[r] - f_N)\Delta T)} e^{j(N-1)(\pi(k\hat{f}[r] - f_N)\Delta T)} \\ \overline{Q}_{k_{DFT}}(\hat{f}[r]) = \frac{\sin(\pi N(k\hat{f}[r] + f_N)\Delta T)}{N \sin(\pi(k\hat{f}[r] + f_N)\Delta T)} e^{-j(N-1)(\pi(k\hat{f}[r] + f_N)\Delta T)} \end{cases} \quad (41)$$

$$\text{half-cycle DFT: } \begin{cases} \overline{P}_{k_{HCF}}(\hat{f}[r]) = \frac{2 \sin(\pi N(k\hat{f}[r] - f_N)\Delta T)}{N \sin(\pi(k\hat{f}[r] - f_N)\Delta T)} e^{j(\frac{N}{2}-1)(\pi(k\hat{f}[r] - f_N)\Delta T)} \\ \overline{Q}_{k_{HCF}}(\hat{f}[r]) = \frac{2 \sin(\pi N(k\hat{f}[r] + f_N)\Delta T)}{N \sin(\pi(k\hat{f}[r] + f_N)\Delta T)} e^{-j(\frac{N}{2}-1)(\pi(k\hat{f}[r] + f_N)\Delta T)} \end{cases} \quad (42)$$

Cosine filter:

$$\begin{cases} \bar{P}_{k\cos}(\hat{f}[r]) = \frac{1}{2N} \left( 1 + je^{-\frac{jN\pi\hat{f}[r]\Delta T}{2}} \left( \frac{\sin(\pi N(k\hat{f}[r] - f_N)\Delta T)}{\sin(\pi(k\hat{f}[r] - f_N)\Delta T)} e^{j(N-1)(\pi(k\hat{f}[r] - f_N)\Delta T)} + \frac{\sin(\pi N(k\hat{f}[r] + f_N)\Delta T)}{\sin(\pi(k\hat{f}[r] + f_N)\Delta T)} e^{j(N-1)(\pi(k\hat{f}[r] + f_N)\Delta T)} \right) \right) \\ \bar{Q}_{k\cos}(\hat{f}[r]) = \frac{1}{2N} \left( 1 + je^{\frac{jN\pi\hat{f}[r]\Delta T}{2}} \left( \frac{\sin(\pi N(k\hat{f}[r] - f_N)\Delta T)}{\sin(\pi(k\hat{f}[r] - f_N)\Delta T)} e^{-j(N-1)(\pi(k\hat{f}[r] - f_N)\Delta T)} + \frac{\sin(\pi N(k\hat{f}[r] + f_N)\Delta T)}{\sin(\pi(k\hat{f}[r] + f_N)\Delta T)} e^{-j(N-1)(\pi(k\hat{f}[r] + f_N)\Delta T)} \right) \right) \end{cases} \quad (43)$$

According to (25) and (26), the fundamental component phasors computed at time samples  $r-1$ ,  $r-2$ ,  $r-3$  and  $r-4$  are:

$$\begin{aligned} \bar{X}_m[r-1] = & \bar{z}^{-1} \bar{P}_1(\hat{f}[r]) \bar{X}_1[r] + \bar{z} \bar{Q}_1(\hat{f}[r]) \bar{X}_1^*[r] \\ & + \bar{z}^{-k} \bar{P}_k(\hat{f}[r]) \bar{X}_k[r] + \bar{z}^k \bar{Q}_k(\hat{f}[r]) \bar{X}_k^*[r] \end{aligned} \quad (44)$$

$$\begin{aligned} \bar{X}_m[r-2] = & \bar{z}^{-2} \bar{P}_1(\hat{f}[r]) \bar{X}_1[r] + \bar{z}^2 \bar{Q}_1(\hat{f}[r]) \bar{X}_1^*[r] \\ & + \bar{z}^{-2k} \bar{P}_k(\hat{f}[r]) \bar{X}_k[r] + \bar{z}^{2k} \bar{Q}_k(\hat{f}[r]) \bar{X}_k^*[r] \end{aligned} \quad (45)$$

$$\begin{aligned} \bar{X}_m[r-3] = & \bar{z}^{-3} \bar{P}_1(\hat{f}[r]) \bar{X}_1[r] + \bar{z}^3 \bar{Q}_1(\hat{f}[r]) \bar{X}_1^*[r] \\ & + \bar{z}^{-3k} \bar{P}_k(\hat{f}[r]) \bar{X}_k[r] + \bar{z}^{3k} \bar{Q}_k(\hat{f}[r]) \bar{X}_k^*[r] \end{aligned} \quad (46)$$

$$\begin{aligned} \bar{X}_m[r-4] = & \bar{z}^{-4} \bar{P}_1(\hat{f}[r]) \bar{X}_1[r] + \bar{z}^4 \bar{Q}_1(\hat{f}[r]) \bar{X}_1^*[r] \\ & + \bar{z}^{-4k} \bar{P}_k(\hat{f}[r]) \bar{X}_k[r] + \bar{z}^{4k} \bar{Q}_k(\hat{f}[r]) \bar{X}_k^*[r] \end{aligned} \quad (47)$$

where  $\bar{z}$  has been defined in (27).

Equations (44)-(47) form a 4x4 linear system whose unknowns are the quantities  $\bar{P}_1(\hat{f}[r]) \bar{X}_1[r]$ ,  $\bar{Q}_1(\hat{f}[r]) \bar{X}_1^*[r]$ ,  $\bar{P}_k(\hat{f}[r]) \bar{X}_k[r]$  and  $\bar{Q}_k(\hat{f}[r]) \bar{X}_k^*[r]$ . Solving for these quantities and substituting in (40), we obtain the following polynomial equation of order  $2k+2$ :

$$a_8 \bar{z}^{-2k+2} + a_7 \bar{z}^{-2k+1} + a_6 \bar{z}^{-2k} + a_5 \bar{z}^{-k+2} + a_4 \bar{z}^{-k+1} + a_3 \bar{z}^{-k} + a_2 \bar{z}^{-2} + a_1 \bar{z} + a_0 = 0 \quad (48)$$

where  $a_i, i=0, \dots, 8$  are the complex coefficients of the polynomial given as follows:

$$a_0 = a_2 = a_6 = a_8 = \bar{X}_m[r-2] \quad (49)$$

$$a_1 = a_3 = a_5 = a_7 = -\bar{X}_m[r-1] - \bar{X}_m[r-3] \quad (50)$$

$$a_4 = \bar{X}_m[r] + 2\bar{X}_m[r-2] + \bar{X}_m[r-4]. \quad (51)$$

Solving the polynomial of (48) for the variable  $\bar{z}$  at each time sample  $r$ , we can compute the exact estimate of instantaneous frequency  $\hat{f}$  in the presence of  $k$ th harmonic through (27), and thus the exact fundamental component

phasor  $\overline{X}_1$  by the following expression, which derives from the solution of the linear system (44)-(47):

$$\begin{aligned} \overline{X}_1[r] = & \left[ \left( \frac{\begin{matrix} -k+4 \\ -z \end{matrix}}{\begin{matrix} -2k+2 & -2k & -k+3 & -k-1 & -2 \\ z & -z & -z & +z & +z & -1 \end{matrix}} \right) \overline{X}_m[r-1] + \left( \frac{\begin{matrix} -2k+4 & -k+3 & -4 \\ z & +z & +z \end{matrix}}{\begin{matrix} -2k+2 & -2k & -k+3 & -k-1 & -2 \\ z & -z & -z & +z & +z & -1 \end{matrix}} \right) \overline{X}_m[r-2] \\ & + \left( \frac{\begin{matrix} -2k+3 & -k+4 & -3 \\ -z & -z & -z \end{matrix}}{\begin{matrix} -2k+2 & -2k & -k+3 & -k-1 & -2 \\ z & -z & -z & +z & +z & -1 \end{matrix}} \right) \overline{X}_m[r-3] + \left( \frac{\begin{matrix} -k+3 \\ z \end{matrix}}{\begin{matrix} -2k+2 & -2k & -k+3 & -k-1 & -2 \\ z & -z & -z & +z & +z & -1 \end{matrix}} \right) \overline{X}_m[r-4] \right] \overline{P}_1(\hat{f}[r])^{-1} \end{aligned} \quad (52)$$

The complex polynomial of (48) is of order  $2k+2$ , which implies that there exist exactly  $2k+2$  complex roots for the variable  $\overline{z}$ . To find the correct root, we can apply the Newton's method and use in each sampling interval  $r$  as an initial guess the complex value  $\overline{z}_0$ , which corresponds to the value of  $\hat{f}$  computed by (36) that considers only the fundamental component. In fact, this initial approximation is rather practical since the contribution of the fundamental component in the value formation of  $\hat{f}$  in the presence of harmonics is by far the most significant, since it is the predominant component encountered in power system voltages and currents. The correct solution of  $\overline{z}$  will lay in the basin of attraction where the initial guess  $\overline{z}_0$  belongs to, and this will ensure very fast convergence of the Newton's method [19].

#### 4.2. Inclusion of other harmonics

Based on the analysis presented in the previous paragraph, we can define the following steps in order to compute the fundamental component phasor  $\overline{X}_1$  in the presence of any number and order of harmonics:

- 1) For each harmonic needed to be considered in the method use two more previously computed phasors  $\overline{X}_m[r-2i+1]$  and  $\overline{X}_m[r-2i]$  where  $i=2, \dots, p$  denotes the ascending number of harmonic and  $p$  stands for the total number of harmonics considered. This will form a  $2p \times 2p$  linear system similar to the linear system (44)-(47).
- 2) Solve the  $2p \times 2p$  linear system for its unknown variables  $\overline{P}_1(\hat{f}[r])\overline{X}_1[r]$ ,  $\overline{Q}_1(\hat{f}[r])\overline{X}_1^*[r]$ , ...,  $\overline{P}_j(\hat{f}[r])\overline{X}_j[r]$ ,  $\overline{Q}_j(\hat{f}[r])\overline{X}_j^*[r]$  where  $j=2, \dots, q$  is the order of harmonic and  $q$  is the maximum order of harmonic considered.
- 3) Substitute the solution of each variable obtained in the previous step in an equation similar to (40) which relates the fundamental component phasor computed by orthogonal FIR filters at time sample  $r$  with the exact phasors

1  $\overline{X}_1, \dots, \overline{X}_q$  at the same sample time. This will lead to a high-order complex polynomial of the variable  $\overline{z}$  like that  
 2 of (48).  
 3  
 4

- 5  
 6 4) Find the correct root of the polynomial by applying at each sampling interval  $r$  the Newton's method using  
 7 Horner's algorithm [20]. To do so, take as an initial estimate,  $\overline{z}_0$ , the result of (27) by using the value of  $\hat{f}$   
 8 calculated by (36).  
 9  
 10 5) Finding the correct solution of  $\overline{z}$  at each sample time  $r$ , calculate the exact value of  $\hat{f}$  in the presence of  
 11 harmonics using (27):  
 12  
 13  
 14  
 15  
 16  
 17

$$18 \hat{f}[r] = \frac{1}{2\pi\Delta T} \cos^{-1}(\operatorname{Re}(\overline{z})). \quad (53)$$

- 19  
 20 6) Combining the solutions for  $\overline{z}$  and  $\hat{f}[r]$  by (53), determine the fundamental component phasor  $\overline{X}_1[r]$  and the  
 21 phasors corresponding to the other harmonics  $\overline{X}_j[r]$  by using expressions similar to (52), which derive from the  
 22 solution of the  $2p \times 2p$  linear system.  
 23  
 24  
 25  
 26  
 27  
 28

29 The use of Newton-Horner's algorithm can be advantageous in a real-time implementation scheme of the extended  
 30 method. Assuming a complex polynomial of degree  $n$ , it requires only  $n$  multiplications and  $n$  additions while the  
 31 classical Newton's method needs  $n(n+1)/2$  multiplications and  $n$  additions, which is a considerable computational  
 32 saving.  
 33  
 34  
 35  
 36  
 37

38 Moreover, the sampling rate selected for the extended method defines the maximum number and order of  
 39 harmonics that can be considered, through the Nyquist theorem. Since the method is intended for power system  
 40 measurement and protection applications, where the sampling rates are in the range of 600 Hz to 1440 Hz, it is  
 41 obvious that a proper sampling rate must be selected. Such a sampling rate would reduce the maximum number of  
 42 harmonics that can be represented in the method and would allow for the number of iterations need to be performed  
 43 in one sampling interval by the Newton's method in order to converge. In that sense, a sampling rate of 12 or 16  
 44 samples per cycle is regarded as a good choice.  
 45  
 46  
 47  
 48  
 49  
 50  
 51  
 52

53 Finally, although we can consider in the method all the harmonics defined by the sampling rate, it is obvious that it  
 54 is computationally efficient to include only those that have the most significant effect among the others (e.g odds  
 55 against even harmonics) or those that affect certain protection functions (e.g. 2nd harmonic in transformer differential  
 56  
 57  
 58  
 59  
 60

protection).

#### 4.3. Performance evaluation through simulation

Three test cases are presented to evaluate the performance of the extended method. The simulation parameter settings are the same as those specified in section 3. Figs. 5-7 refer to a constant frequency deviation case where a 3rd harmonic component has been added to the pure sinusoidal signal. The Cosine filter is employed for fundamental phasor computation. Figs. 8-10 correspond to a frequency variation case where a combination of 3rd and 5th harmonic has been superimposed on the pure sinusoidal signal. The half-cycle DFT filter is used for phasor extraction. Fig. 11 shows the performance of the extended compensation method with respect to a noisy input signal. The measured phasor is provided by the full-cycle DFT filter.

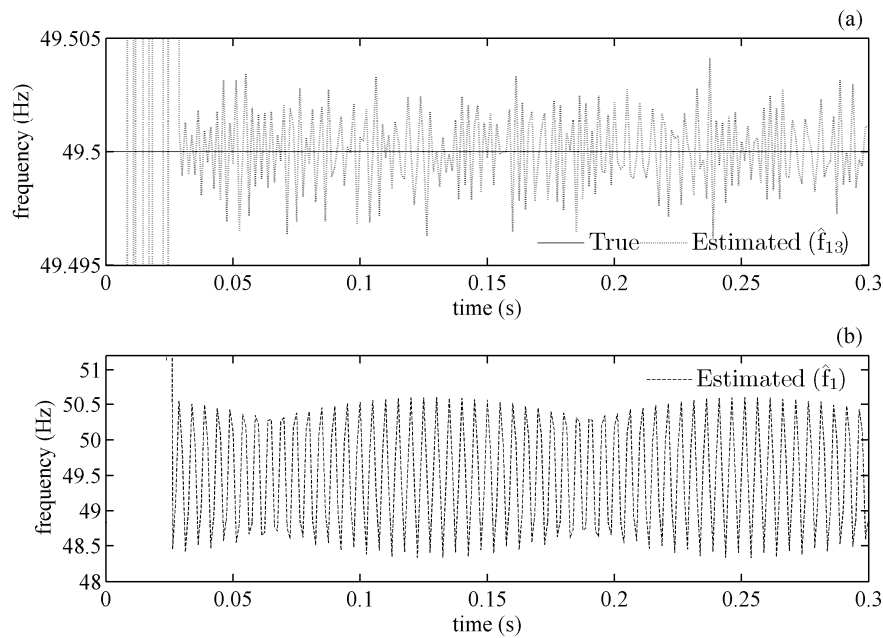


**Fig. 5.** (a) True and estimated frequency  $\hat{f}_{13}$ . (b) Estimated frequency  $\hat{f}_1$  (test signal:

$$x(t) = \cos(2\pi 49.5t) + 0.1\cos(6\pi 49.5t), \quad f(t) = 49.5 \text{ Hz}.$$

In Appendix, we provide the polynomial needed to be solved along with the analytical expression required for obtaining the exact fundamental component phasor in the case that both the 3rd and 5th harmonics are considered in the extended method. For the case of the 3rd harmonic only, these are easily obtained from (48) and (52) by using  $k = 3$ .

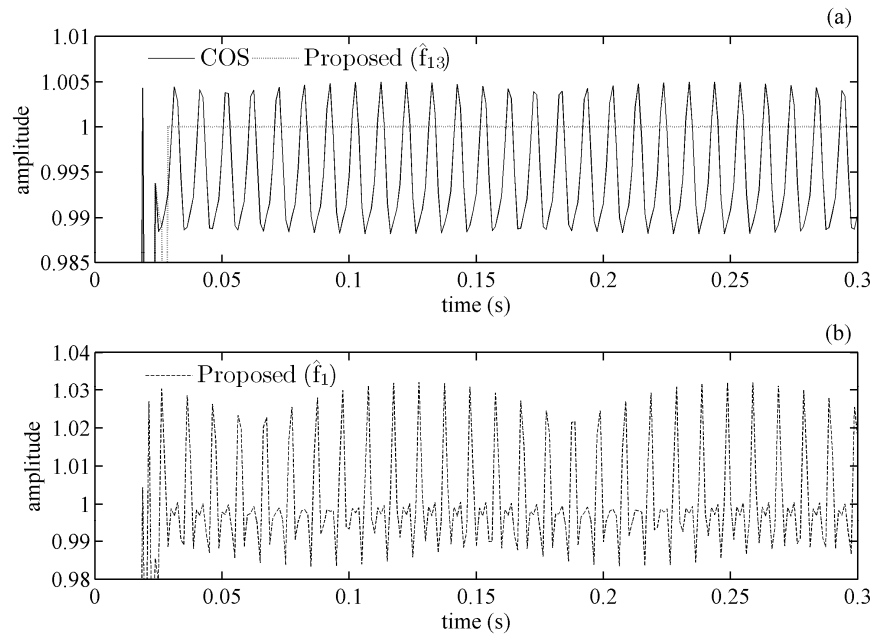


**Fig. 6.** (a)-(b) Comparison of amplitude computation performances of the Cosine filter and the two versions of the extended method that use  $\hat{f}_{13}$  and  $\hat{f}_1$  respectively (test signal:  $x(t) = \cos(2\pi 49.5t) + 0.1\cos(6\pi 49.5t)$ ,  $f(t) = 49.5$  Hz).

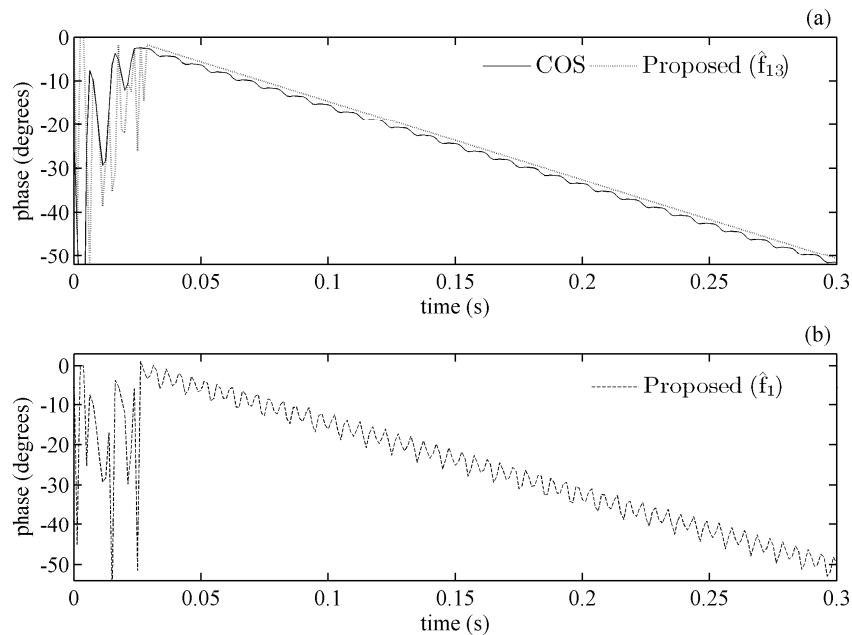


**Fig. 7.** (a)-(b) Comparison of phase angle computation performances of the Cosine filter and the two versions of the extended method that use  $\hat{f}_{13}$  and  $\hat{f}_1$  respectively (test signal:  $x(t) = \cos(2\pi 49.5t) + 0.1\cos(6\pi 49.5t)$ ,  $f(t) = 49.5$  Hz).

Figs. 5(a),(b) show the simulation results for the estimated frequencies  $\hat{f}_1$  and  $\hat{f}_{13}$  which correspond to the

1 solution of  $\hat{f}$  obtained by the extended method considering only the fundamental and both the 3rd harmonic  
2 respectively. It can be seen that  $\hat{f}_{13}$  gives very accurate estimates of the actual signal frequency, while the quantity  
3  $\hat{f}_1$  has errors because its calculation does not take into account the effect of the 3rd harmonic. Moreover, the errors  
4 in  $\hat{f}_1$  introduce errors in the estimated phasor, both in terms of its amplitude and phase angle, as shown in Figs. 6(b)  
5 and 7(b). On the other hand, the extended method with inclusion of the 3rd harmonic compensates fully the errors  
6 produced by the Cosine filter and provides accurate phasor estimates, as can be observed in Figs. 6(a) and 7(a)  
7 respectively.

8  
9  
10  
11  
12  
13  
14  
15  
16  
17  
18  
19 Similar observations can be made in Figs. 8-10. Figs. 8(a),(b),(c) show that while the estimated frequency  $\hat{f}_{135}$ ,  
20 which encompasses both the effect of the 3rd and 5th harmonic, tracks very effectively the actual signal frequency,  
21 the estimates  $\hat{f}_1$  and  $\hat{f}_{13}$  fail to do so. This has a direct effect on both the amplitude and phase angle results produced  
22 by the extended method with inclusion of the fundamental only and both the 3rd harmonic, although the latter has  
23 superior performance against the former, as illustrated in Figs. 9(b),(c) and Figs. 10(b),(c) respectively. Only the  
24 extended method with inclusion of the 5th harmonic also succeeds to provide accurate phasor estimates and cancels  
25 out the errors introduced by the half-cycle DFT, as shown in Figs. 9(a) and 10(a). However, this is at the expense of  
26 some additional time delay since more previously computed phasors by HCFT are needed.

27  
28  
29  
30  
31  
32  
33  
34  
35  
36  
37 We know that if a method can be used in real world, it must take noise into consideration. The frequency of test  
38 signal in Fig. 11 is 49.5 Hz, and we have added a 3rd harmonic of 10% and white zero-mean Gaussian noise with a  
39 signal-to-noise ratio (SNR) of 60 dB. It can be seen in Fig. 11(a) that, contrary to  $\hat{f}_1$  which does not account for the  
40 third harmonic, the estimated frequency  $\hat{f}_{13}$  yields fairly accurate results. Fluctuations around the true value are due  
41 to the noise in the input signal. If better accuracy is desirable, this effect of noise could be further reduced by using  
42 appropriate smoothing filter (e.g. moving average filter). However, it must be noted that these actions will increase  
43 the response time of the method. Finally, in Fig. 11(b) and 11(c), it is observed that the errors of the full-cycle DFT  
44 and the proposed method with inclusion of the fundamental component only are larger than the extended method  
45 with inclusion of 3<sup>rd</sup> harmonic also, in terms of phasor magnitude and phase angle.

46  
47  
48  
49  
50  
51  
52  
53  
54  
55  
56  
57 In all simulation examples as well as in others experiments performed, it was found that the Newton's method  
58 requires four iterations maximum to converge if a margin of  $10^{-6}$  is selected. This is very promising as far as it  
59  
60

concerns the real-time implementation of the method and it is an indication that the initial approximation assumed is rather practical.

## 5. Conclusion

In this paper, a method is presented that provides accurate phasor measurements during frequency variations in power systems. This is achieved by correcting the errors produced by orthogonal FIR filters in phasor computation through an accurate estimate of the local instantaneous frequency, which is obtained with a recursive procedure that is concurrent with the phasor computation process. The theoretical aspects of the method have been discussed thoroughly and the simulation results validate the merits of the proposed method: it is easy to implement, accurate and deals effectively with harmonics and noise. Although a real-time implementation of the method has not been done yet, certain suggestions have been made to this direction.

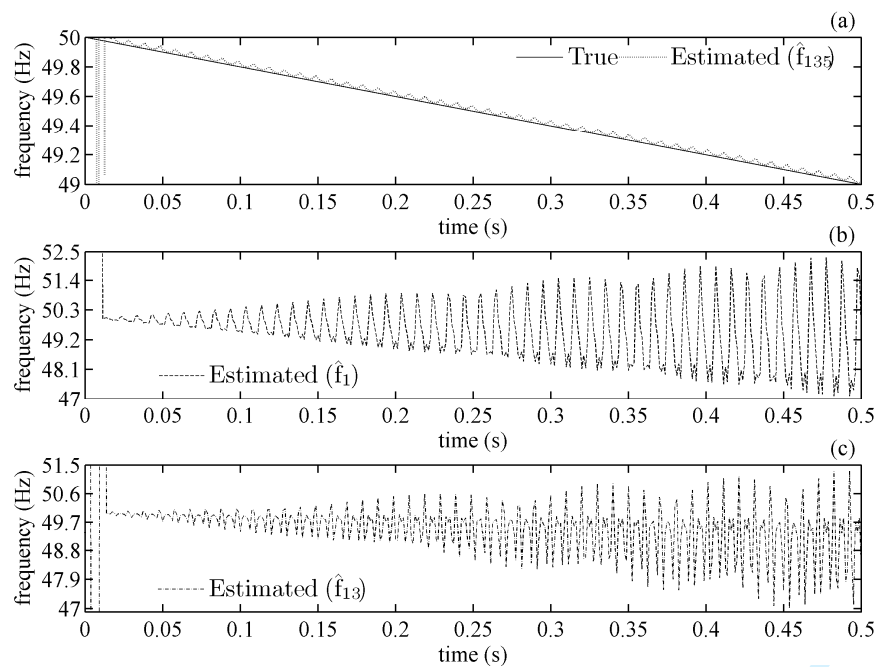


**Fig. 8.** (a) True and estimated frequency  $\hat{f}_{135}$ . (b) Estimated frequency  $\hat{f}_1$ . (c) Estimated frequency  $\hat{f}_{13}$  (test signal:

$$x(t) = \cos(2\pi(50t - t^2)) + 0.15\cos(6\pi(50t - t^2)) + 0.03\cos(10\pi(50t - t^2)), f(t) = 50 - 2t \text{ Hz}.$$

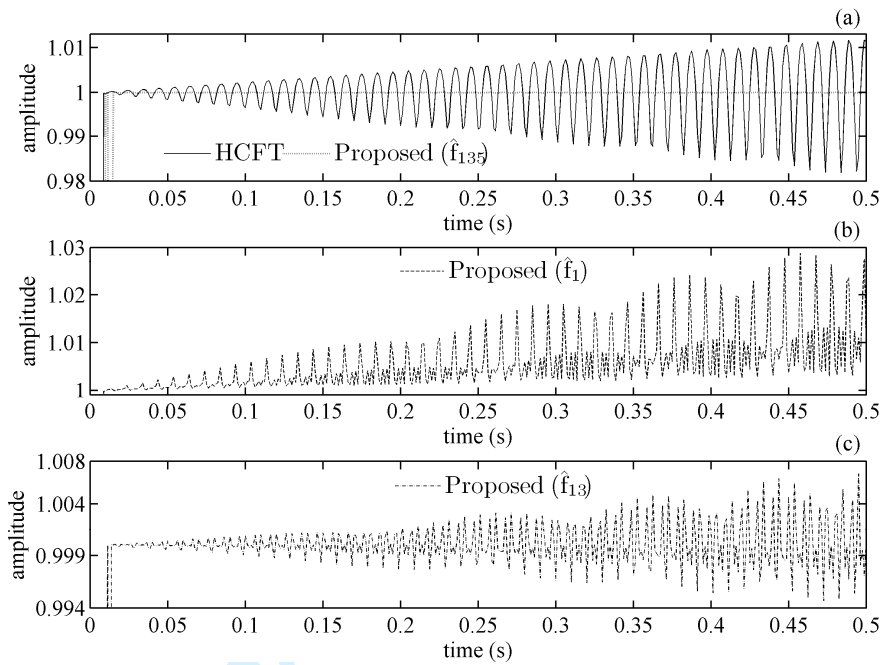


**Fig. 9.** (a),(b),(c) Comparison of amplitude computation performances of the half-cycle DFT and the three versions of the extended method that correspond to the quantities  $\hat{f}_{135}$ ,  $\hat{f}_1$  and  $\hat{f}_{13}$  respectively (test signal:  $x(t)=\cos(2\pi(50t-t^2))+0.15\cos(6\pi(50t-t^2))+0.03\cos(10\pi(50t-t^2))$ ,  $f(t)=50-2t$  Hz).

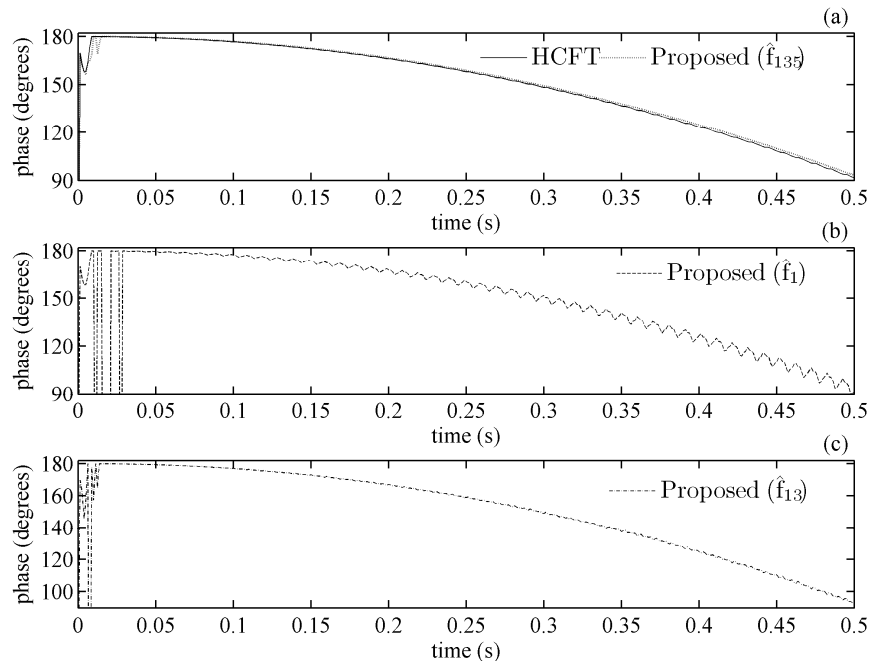


**Fig. 10.** (a),(b),(c) Comparison of phase angle computation performances of the half-cycle DFT and the three versions of the extended method that correspond to the quantities  $\hat{f}_{135}$ ,  $\hat{f}_1$  and  $\hat{f}_{13}$  respectively (test signal:  $x(t)=\cos(2\pi(50t-t^2))+0.15\cos(6\pi(50t-t^2))+0.03\cos(10\pi(50t-t^2))$ ,  $f(t)=50-2t$  Hz).

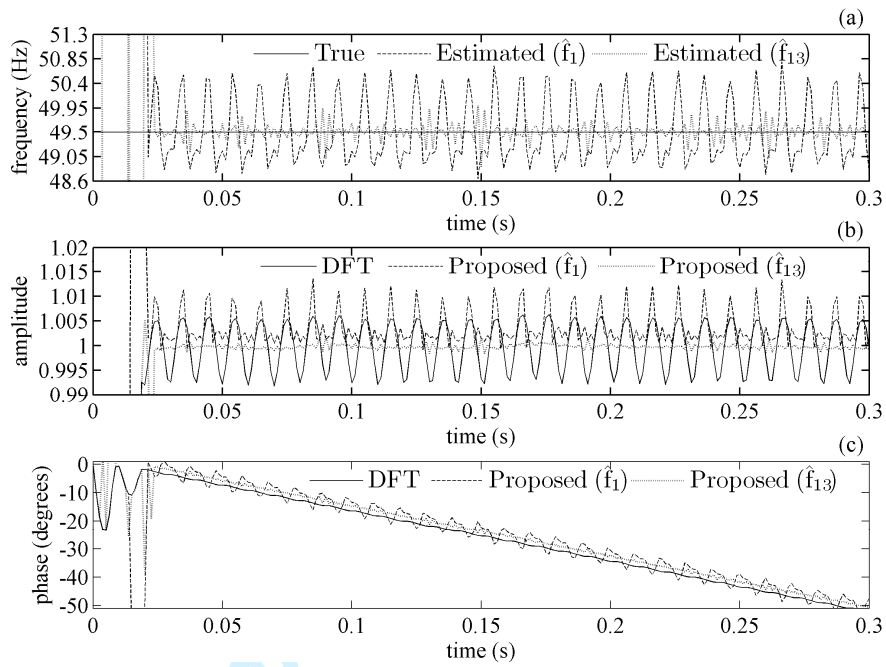


**Fig. 11.** (a) True and estimated frequency  $\hat{f}$  (b) Comparison of amplitude computation performances of the full-cycle DFT and the two versions of the extended method which correspond to the quantities  $\hat{f}_1$  and  $\hat{f}_{13}$  respectively. (c) Comparison of phase angle computation performances of the full-cycle DFT and the two versions of the extended method (test signal:  $x(t)=\cos(2\pi 49.5t)+0.1\cos(6\pi 49.5t)$ , with SNR=60 dB).

## Appendix

Following are the precalculated equations that apply for the extended method which considers both the influence of the 3rd and 5th harmonic. The high-order polynomial of  $\bar{z}$  is as:

$$a_{18}\bar{z}^{-18} + a_{17}\bar{z}^{-17} + a_{16}\bar{z}^{-16} + a_{15}\bar{z}^{-15} + a_{14}\bar{z}^{-14} + a_{13}\bar{z}^{-13} + a_{12}\bar{z}^{-12} + a_{11}\bar{z}^{-11} + a_{10}\bar{z}^{-10} + a_9\bar{z}^{-9} + a_8\bar{z}^{-8} + a_7\bar{z}^{-7} + a_6\bar{z}^{-6} + a_5\bar{z}^{-5} + a_4\bar{z}^{-4} + a_3\bar{z}^{-3} + a_2\bar{z}^{-2} + a_1\bar{z}^{-1} + a_0 = 0 \quad (A1)$$

where  $a_i, i=0, \dots, 18$  are its complex coefficients given by the following equations:

$$a_0 = a_2 = a_{16} = a_{18} = \bar{X}_m[r-3] \quad (A2)$$

$$a_1 = a_3 = a_{15} = a_{17} = -\bar{X}_m[r-2] - \bar{X}_m[r-4] \quad (A3)$$

$$a_4 = a_{14} = \bar{X}_m[r-1] + 2\bar{X}_m[r-3] + \bar{X}_m[r-5] \quad (A4)$$

$$a_5 = a_7 = a_{11} = a_{13} = -2\bar{X}_m[r-2] - 2\bar{X}_m[r-4] \quad (A5)$$

$$a_6 = a_8 = a_{10} = a_{12} = \bar{X}_m[r-1] + 3\bar{X}_m[r-3] + \bar{X}_m[r-5] \quad (A6)$$

$$a_9 = -\overline{X}_m[r] - 3\overline{X}_m[r-2] - 3\overline{X}_m[r-4] - \overline{X}_m[r-6] \quad (A7)$$

The fundamental component phasor at each sample time  $r$  is calculated by:

$$\begin{aligned} \overline{X}_1[r] = & \left( \frac{\overline{z}^{-13}}{\overline{z}^{-18} \overline{z}^{-16} \overline{z}^{-14} \overline{z}^{-12} \overline{z}^{-10} \overline{z}^{-8} \overline{z}^{-6} \overline{z}^{-4} \overline{z}^{-2} \overline{z}^{-1}}{\overline{z}^{-18} \overline{z}^{-16} \overline{z}^{-14} \overline{z}^{-12} \overline{z}^{-10} \overline{z}^{-8} \overline{z}^{-6} \overline{z}^{-4} \overline{z}^{-2} \overline{z}^{-1}} \right) \overline{X}_m[r-1] + \left( \frac{\overline{z}^{-8} \overline{z}^{-10} \overline{z}^{-12} \overline{z}^{-16} \overline{z}^{-18}}{\overline{z}^{-18} \overline{z}^{-16} \overline{z}^{-14} \overline{z}^{-12} \overline{z}^{-10} \overline{z}^{-8} \overline{z}^{-6} \overline{z}^{-4} \overline{z}^{-2} \overline{z}^{-1}} \right) \overline{X}_m[r-2] \\ & + \left( \frac{\overline{z}^{-5} \overline{z}^{-7} \overline{z}^{-9} \overline{z}^{-11} \overline{z}^{-13} \overline{z}^{-15} \overline{z}^{-17} \overline{z}^{-21}}{\overline{z}^{-18} \overline{z}^{-16} \overline{z}^{-14} \overline{z}^{-12} \overline{z}^{-10} \overline{z}^{-8} \overline{z}^{-6} \overline{z}^{-4} \overline{z}^{-2} \overline{z}^{-1}} \right) \overline{X}_m[r-3] + \left( \frac{\overline{z}^{-4} \overline{z}^{-8} \overline{z}^{-10} \overline{z}^{-12} \overline{z}^{-14} \overline{z}^{-16} \overline{z}^{-18} \overline{z}^{-20}}{\overline{z}^{-18} \overline{z}^{-16} \overline{z}^{-14} \overline{z}^{-12} \overline{z}^{-10} \overline{z}^{-8} \overline{z}^{-6} \overline{z}^{-4} \overline{z}^{-2} \overline{z}^{-1}} \right) \overline{X}_m[r-4] \\ & + \left( \frac{\overline{z}^{-7} \overline{z}^{-9} \overline{z}^{-13} \overline{z}^{-15} \overline{z}^{-17}}{\overline{z}^{-18} \overline{z}^{-16} \overline{z}^{-14} \overline{z}^{-12} \overline{z}^{-10} \overline{z}^{-8} \overline{z}^{-6} \overline{z}^{-4} \overline{z}^{-2} \overline{z}^{-1}} \right) \overline{X}_m[r-5] + \left( \frac{\overline{z}^{-12}}{\overline{z}^{-18} \overline{z}^{-16} \overline{z}^{-14} \overline{z}^{-12} \overline{z}^{-10} \overline{z}^{-8} \overline{z}^{-6} \overline{z}^{-4} \overline{z}^{-2} \overline{z}^{-1}} \right) \overline{X}_m[r-6] \left[ \hat{P}_1(\hat{f}[r])^{-1} \right]. \end{aligned} \quad (A8)$$

## References

- [1] E. O. Schweitzer III, D. Hou, "Filtering for protective relays," in: The 47th Annual Georgia Tech Protective Relay Conference, Atlanta, GA, 1993.
- [2] A. G. Phadke, J. S. Thorp, Synchronized Phasor Measurements and Their Applications, New York: Springer, 2008.
- [3] D. Hou, "Relay element performance during power system frequency excursions," in: The 61st Annual Conference for Protective Relay Engineers, College Station, TX, 2008.
- [4] A. G. Phadke, B. Kasztenny, "Synchronized phasor and frequency measurement under transient conditions," IEEE Trans. Power Del., vol. 24, no. 1, pp. 89-95, January 2009.
- [5] Working Group I16 of the Relaying Practices Subcommittee of the IEEE Power System Relaying Committee, "Understanding Microprocessor-Based Technology Applied to Relaying," Technical Report, 2004 [Online]. Available: <http://www.pes-psrc.org/i/I16/>.
- [6] B. Boashash, "Estimating and interpreting the instantaneous frequency of a signal: Part I: Fundamentals, Part II: Algorithms and applications," Proc. IEEE, vol. 80, no. 4, pp. 520-568, April 1992.
- [7] A. G. Phadke, J. S. Thorp, M. Adamiak, "A new measurement technique for tracking voltage phasors, local system frequency, and rate of change of frequency," IEEE Trans. Power App. Syst., vol. 102, no. 5, pp. 1025-1038, May 1983.
- [8] M. M. Begovic, P. M. Djuric, S. Dunlap, A. G. Phadke, "Frequency tracking in power networks in the presence of harmonics," IEEE Trans. Power Del., vol. 8, no. 2, pp. 480-486, April 1993.

- 1  
2  
3  
4  
5  
6  
7  
8  
9  
10  
11  
12  
13  
14  
15  
16  
17  
18  
19  
20  
21  
22  
23  
24  
25  
26  
27  
28  
29  
30  
31  
32  
33  
34  
35  
36  
37  
38  
39  
40  
41  
42  
43  
44  
45  
46  
47  
48  
49  
50  
51  
52  
53  
54  
55  
56  
57  
58  
59  
60
- [9] G. Benmouyal, "An adaptive sampling-interval generator for digital relaying," IEEE Trans. Power Del., vol. 4, no. 3, pp. 1602-1609, July 1989.
- [10] D. Hart, D. Novosel, Y. Hu, B. Smith, M. Egolf, "A new frequency tracking and phasor estimation algorithm for generator," IEEE Trans. Power Del., vol. 12, no. 3, pp. 1064-1073, July 1997.
- [11] T. Sidhu, "Accurate measurement of power system frequency using a digital signal processing technique," IEEE Trans. Instrum. Meas., vol. 48, no. 1, pp. 75-81.
- [12] J. Z. Yang, C. W. Liu, "A precise calculation of power system frequency and phasor," IEEE Trans. Power Del., vol. 15, no. 2, pp. 494-499, April 2000.
- [13] A. A. Girgis, T. L. D. Hwang, "Optimal estimation of voltage phasors and frequency deviation using linear and nonlinear kalman filter: Theory and limitations," IEEE Trans. Power App. Sys., vol. 103, no. 10, pp. 2943-2949, October 1984.
- [14] I. Kamwa, R. Grondin, "Fast adaptive schemes for tracking voltage phasor and local frequency in power transmission and distribution systems," IEEE Trans. Power Del., vol. 7, no. 2, pp. 789-795, April 1992.
- [15] V. V. Terzija, M. B. Djuric, B. D. Kovacevic, "Voltage phasor and local system frequency estimation using Newton-type algorithm," IEEE Trans. Power Del., vol. 9, no. 3, pp. 1368-1374, July 1994.
- [16] J. A. de la O Serna, "Dynamic phasor estimates for power system oscillations," IEEE Trans. Instrum. Meas., vol. 56, no. 5, pp. 1648-1657, October 2007.
- [17] W. Premerlani, B. Kasztenny, M. Adamiak, "Development and implementation of a synchrophasor estimator capable of measurements under dynamic conditions," IEEE Trans. Power Del., vol. 23, no. 1, pp. 109-123, January 2008.
- [18] G. Benmouyal, "System and method for exact compensation of fundamental phasors," U.S. Patent 6,934,654, August 2005.
- [19] W. H. Press, S. A. Teukolsky, W. T. Vetterling, B. P. Flannery, Numerical recipes: The Art of Scientific Computing, Cambridge University Press, 2007.
- [20] G. A. Sitton, C. S. Burrus, J. W. Fox, S. Treitel, "Factoring very-high-degree polynomials," IEEE Signal Process. Mag., vol. 20, no. 6, pp. 27-42, November 2003.